J Mater Sci (2013) 48:1225–1230
DOI 10.1007/s10853-012-6863-7

Influence of oxygen partial pressure on structural, electrical, and optical properties of Al-doped ZnO film prepared by the ion beam co-sputtering method

Yu-Yun Chen · Jin-Cherng Hsu · Chun-Yi Lee · Paul W. Wang

Received: 9 April 2012 / Accepted: 3 September 2012 / Published online: 19 September 2012

Abstract Aluminum doped zinc oxide (AZO) films were prepared at room temperature by ion beam co-sputtering system under various oxygen partial pressures. The structural, electrical, and optical properties of the films were studied by XRD, XPS, Hall measurement, and spectrometer. The AZO film with low resistivity, 7.8×10^{-4} Ω cm, and high transparency, ~80 %, was obtained at the optimum oxygen partial pressure of 1.3×10^{-4} Torr and the intense (002) diffraction peak was observed simultaneously. Different optical band gaps observed in the films prepared under various oxygen partial pressures are closely related to the carrier concentrations in the films. Three O_{1s} components were applied to fit the XPS O_{1s} spectra. They consist of adsorbed oxygen species, oxygen in O-Zn bonds surrounded by oxygen vacancies, and oxygen in the O-Zn bonds. Two components, Zn in Zn–O bonds and Zn with higher than +2 oxidation states, were used to fit $Zn_{2p3/2}$ spectra. It was found that the increase of film's resistivity which may result from the drops in the oxygen vacancy, Zn interstitial, carrier concentration, and grain size. No apparent transmission change of the film in the visible light region as a function of oxygen partial pressure was detected.

Y.-Y. Chen
Graduate Institute of Applied Science and Engineering, Fu Jen Catholic University, 510 Chung-Cheng Rd., Hsinchuang, New Taipei City 24205, Taiwan
e-mail: 497598028@mail.fju.edu.tw

J.-C. Hsu · C.-Y. Lee
Department of Physics, Fu Jen Catholic University, 510 Chung-Cheng Rd., Hsinchuang, New Taipei City 24205, Taiwan
e-mail: 054326@mail.fju.edu.tw

C.-Y. Lee
e-mail: johnny521203@hotmail.com

P. W. Wang (✉)
Department of Physics, Bradley University, 1501 W. Bradley Ave., Peoria, IL 61625, USA
e-mail: pwang@fsmail.bradley.edu

Introduction

ZnO with wide band gap of 3.3 eV and large exciton binding energy of 60 meV has been widely studied and used in many technological applications. The transparent conducting films, Al-doped ZnO (AZO), with high electrical conductivity and high transparency in the visible light region have been extensively applied in electrical and optical applications such as solar cells, flat panel displays, anode contact for organic light-emitting diodes, and electro-optical devices. From other reports, it was found that the deposition condition plays the crucial factor to influence the microstructure, optical and electrical properties of the films. There are many methods used for the preparation of AZO films such as RF or DC [1–3] magnetron sputtering [4–6], pulsed-laser deposition (PLD) [7, 8], sol–gel process [9], and spray pyrolysis [10].

The ion beam sputtering deposition (IBSD) used in this work is a relatively unique method in which a high packing-density film can be fabricated by the IBSD with atom-by-atom or molecule-by-molecule transport growth mechanism at low substrate temperature [11, 12]. The high quality AZO films with an optimum aluminum component were easily fabricated as both Zn and Al targets were co-sputtered by an energetic ion beam as reported previously [13, 14]. The influence of oxygen partial pressure during deposition process on the physical properties of AZO films is important since the oxygen vacancies were attributed to the photoluminescence and played as electrical donors in

the ZnO films [15–21]. In most of sputtering deposition methods, the oxide ceramic targets are usually used to deposit the films to prevent losing the oxygen atoms in the films which results in the worse properties of AZO films. Therefore, in order to investigate a particular role of oxygen in the AZO films, various oxygen partial pressures were used when both Zn and Al metallic targets were sputtered by argon ions during the film fabrication.

It is known that the resistivity of the AZO film can be adjusted by the deposition conditions (for example, [22]); however, it is still debatable how the resistivity actually correlated to the structure and defects in the film. In this study, structural, electrical, and optical properties of the AZO films prepared under various partial oxygen pressures were investigated to understand how property modifications due to the structure changes caused by various oxygen partial pressures. Different optical band gaps observed in the films prepared under various oxygen partial pressures are closely related to the carrier concentrations in the films. Furthermore, the conductivity of the film was dependent on the crystallinity, grain size, carrier concentration, oxygen vacancies, and zinc interstitials.

Experiments

The AZO films were deposited on the B270 glass substrate with the size of 1.3 cm × 1.3 cm by ion beam co-sputtering process at room temperature. Both metallic targets Zn and Al with purity of 99.99 % mounted side by side on a water-cooling copper block were sputtered by the high energetic argon ion beam during the deposition. The glass substrates were cleaned by ethanol in an ultrasonic cleaner and blown dry by nitrogen gas prior to the deposition. A base pressure of 4.0×10^{-6} Torr was achieved using a cryopump. Then, the argon working gas and the oxygen ambient gas were fed into the ion source and the chamber, respectively. The ion beam voltage was kept at 1000 V with the ion beam current of 20 mA. Four different oxygen partial pressures of 1.0×10^{-4}, 1.3×10^{-4}, 1.7×10^{-4}, and 2.0×10^{-4} Torr were used and the total pressure of the chamber was kept at 2.4×10^{-4} Torr during the deposition. The detailed experimental set-up can be found in our previous publication [13]. The aluminum concentrations in the films were maintained at 1.5 atomic % and determined by Energy-dispersive X-ray spectroscopy. The transmission spectra of AZO films fabricated under variation of oxygen partial pressures were measured by UV–Visible-Near IR spectrometer (Cary 5E). An X-ray diffraction (XRD) apparatus (Rigaku Multiflex) with a Cu Kα line (1.54055 Å) was used to characterize the structure of AZO films. The resistivity, carrier concentration and carrier mobility were measured at room temperature by Hall measurement with the Van der Pauw method. The chemical compositions and states of the elements in the film were characterized at room temperature by X-ray photoelectron spectroscopy (XPS) apparatus (Perkin-Elmer PHI1600).

Results and discussion

The structure of AZO films characterized by XRD with respect to the different oxygen partial pressures is shown in Fig. 1. The (001) and (002) ZnO diffraction peaks were detected in the films, and the most intense (002) peak was obtained in the film prepared under the oxygen partial pressure of 1.3×10^{-4} Torr. The obvious (002) peaks shown in the XRD patterns indicate that AZO films have a high texture of the crystalline (002) orientation along the c-axis perpendicular to the substrate surface. Since the peak intensity is closely related to the crystallinity of the film, the higher the oxygen partial pressure, the lower the crystallinity of the film in general. Apparently, a film with better crystallinity resulting in lowest resistivity, as reported previous [13], can be prepared under the oxygen pressure of 1.3×10^{-4} Torr.

The grain size and atomic d-spacing of AZO films calculated by Scherrer's formula and Bragg's diffraction condition, respectively, as functions of oxygen partial pressures are plotted in Fig. 2. As the oxygen partial pressure increasing, the worse structure in the film is produced in general due to the poor crystallinity with the smaller grains while the d-spacing remains about the same first and then increases little when the pressure is equal or higher than 1.7×10^{-4} Torr. It means that the number of Al^{3+} ions replacing the Zn^{2+} ions in AZO structure is reduced and the compressive stress in the films, which can be calculated from the difference between the lattice

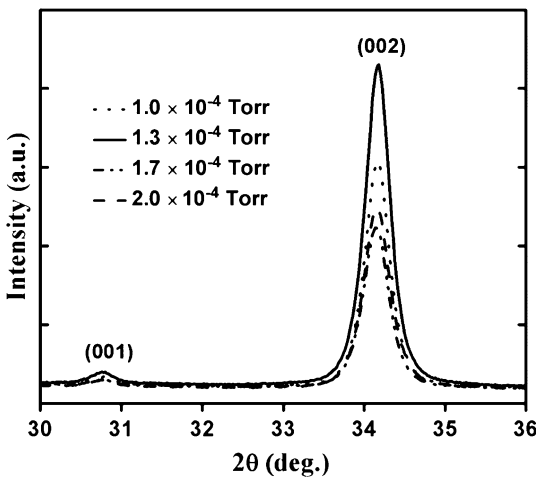

Fig. 1 The XRD patterns of AZO films prepared at different oxygen partial pressure

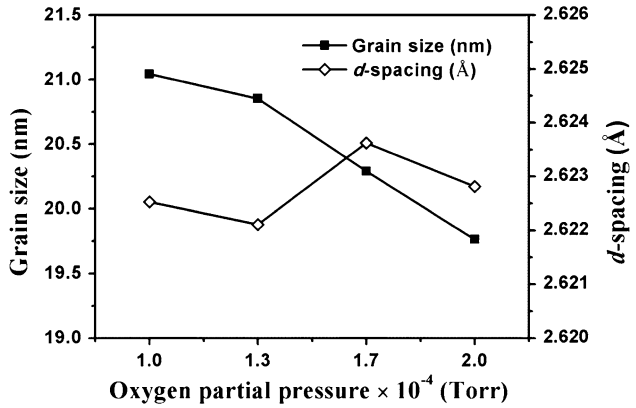

Fig. 2 The grain size and atomic d-spacing of AZO films were plotted as functions of oxygen partial pressures

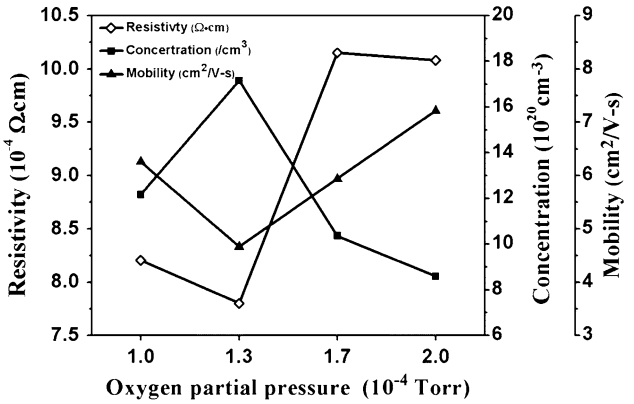

Fig. 3 The electrical properties of AZO films was measured with respect to oxygen partial pressure

constant of ZnO and d-spacing [14], increases little as the oxygen partial pressure increases. The bigger d-spacing in AZO film indicates that less Al atoms replace the Zn atoms in the lattice due to the smaller ionic radius of Al^{3+} (53–67.5 pm) than that of Zn^{2+} (74–104 pm) such that the resistivity increases [13, 23]. The extrinsic defects in the ZnO films due to the Al impurity play as donors in the films since each Al^{3+} ion donates an extra electron compared to Zn^{2+} ion in ZnO structure. Therefore, the donor concentration reduces little as oxygen pressure increases. Moreover, from our previous study [13], the smaller the grain size in the film, the higher the scattering at the boundary, and hence the higher the resistivity.

In ZnO film intrinsic defects, oxygen vacancies and zinc interstitials, act as donors to produce carrier electrons, influence the electrical and optical properties as the carrier concentration is modified. [20, 21, 24–26]. In order to understand the relationship between oxygen pressure and electrical property of the film, the resistivity, carrier concentration and carrier mobility were measured by Hall measurement with the Van der Pauw method, and the results are shown in Fig. 3. All the films were shown n-type semiconductors after Hall measurements. It is well known that the resistivity is proportional to the reciprocal product of carrier concentration and mobility. In Fig. 3, it is found that the carrier concentration increases first and then drops to a value of $8.58 \times 10^{20}/cm^3$ as the oxygen partial pressure is increased. Moreover, the carrier mobility decreases initially and then increases as the oxygen gas increases further. It was observed that the trend of carrier concentration was opposite to that of mobility in the pattern when the oxygen partial pressure increased. The low carrier concentration and the high carrier mobility seen as the oxygen partial pressure increasing can be attributed to the defects in the film. The charge carriers, electrons, generated by the oxygen vacancy/zinc interstitial donors decreased as the oxygen partial pressure increased which was seen in XPS spectra shown below. The lowest resistivity, 7.8×10^{-4} Ω cm, due to the overall effect of both concentration and mobility was obtained in the film prepared under 1.3×10^{-4} Torr. Combined to the intense (002) peak in Fig. 1 and the resistivity results the optimum oxygen partial pressure to deposit the AZO film with lowest resistivity and highest crystallinity is 1.3×10^{-4} Torr in this study.

The optical spectra of AZO films prepared under different oxygen partial pressures measured by spectrometer were plotted in Fig. 4. In the visible light range, the transmittance of AZO films is above 80 % in average regardless of the oxygen partial pressure. The transmittance falls sharply due to the band-to-band absorption in the UV wavelength region. It shows that the different oxygen partial pressures have no significant influence on the transmittance in the range of visible light but the absorption edge of AZO films does shift toward the longer wavelength when the oxygen pressure is higher than 1.3×10^{-4} Torr. The shift is caused by Burstein-Moss effect influenced by the carrier concentrations in the film.

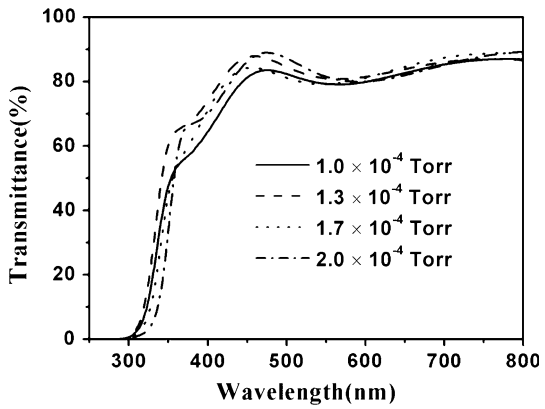

Fig. 4 The optical spectra of AZO films with different oxygen partial pressure were observed

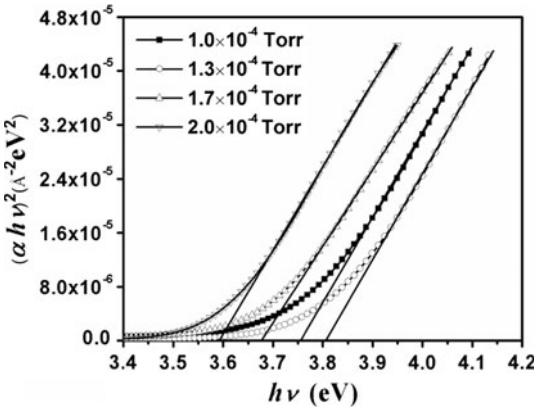

Fig. 5 Plot of $(\alpha hv)^2$ as a function of hv of AZO films to determine the optical energy *band gap* of the film

Using the relation between $(\alpha hv)^2$ and hv for the AZO films prepared under different oxygen partial pressures, the optical band gap can be determined and the results are shown in Fig. 5, where α is the absorption coefficient. The optical band gap was obtained using the extrapolation from the plots of $(\alpha hv)^2$ versus hv and the numerical values of the optical band gap for the AZO films with the increase of oxygen partial pressure are 3.76, 3.81, 3.68, and 3.60 eV. According to the Burstein-Moss effect, the optical band gap widening is directly proportional to the 2/3 power of the carrier concentration of the film [14]. Therefore, the absorption edge shifts to the longer wavelength with increasing oxygen partial pressure as a result of the decrease of the carrier concentration in the film.

From the results of optical, structural, and electrical properties of the films it was confirmed again that the low resistivity and high transparency of AZO films prepared at room temperature by the IBSD method can be obtained with an optimum oxygen partial pressure.

To study the film's surface compositions and chemical bonding environment XPS is applied. Since both the Al concentrations, 1.5 at.%, and the atomic sensitivity factor of XPS Al_{2p} signal, 0.11[27], were so low that no clear Al signal was detected by XPS. The XPS O_{1s} and $Zn_{2p3/2}$ spectra were shown in Figs. 6 and 7, respectively. The $Zn_{2p3/2}$ signal can be fitted by two components centered at 1021.5 and 1022.3 eV. The dominant low binding energy (BE) component (ZnI) can be assigned to either the Zn atoms in the Zn–O bonds. [19, 28] or the Zn with 2 + oxidation state. The high BE component (ZnII) can be assigned to either the Zn in the Zn–O bonds surrounded by oxygen vacancies or the Zn with higher than 2 + oxidation state. Because the ZnII are Zn atoms not exactly occupied in the lattice site of regular Zn ions, they may be related to the Zn interstitials. The ZnI first decreased little in 1.3×10^{-4} Torr film and then increased as the oxygen

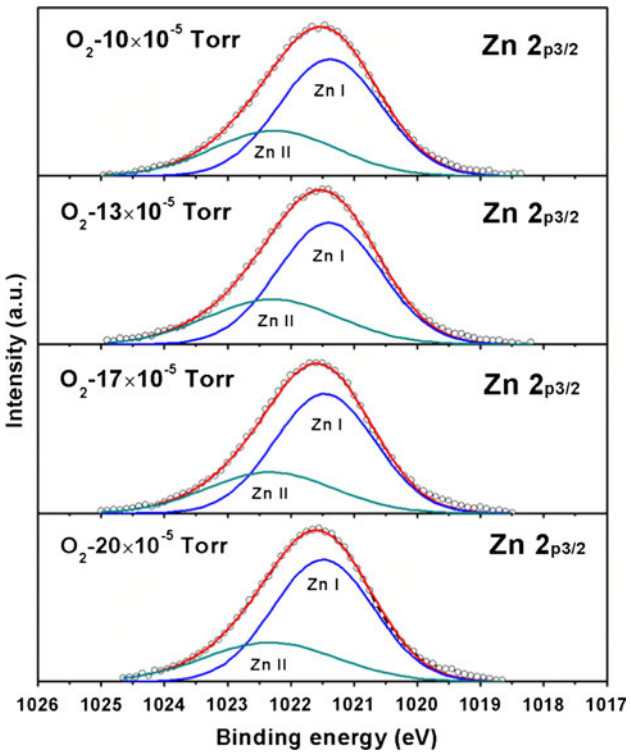

Fig. 6 The original and fitted XPS spectra of $Zn_{2p3/2}$, two components centered at 1021.5 and 1022.3 eV were used to fit the spectra

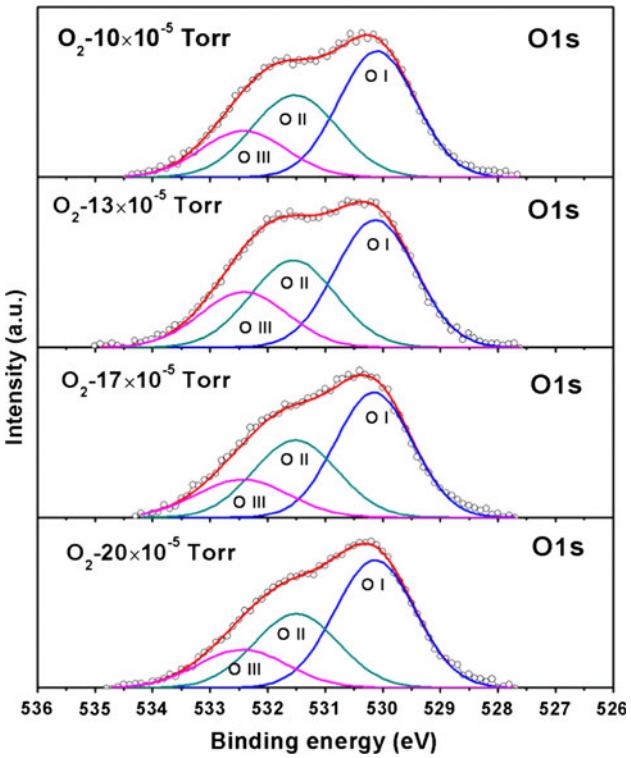

Fig. 7 The original and fitted XPS spectra of O_{1s}, three components were applied, 530.12 ± 0.02, 531.47 ± 0.03 and 532.45 ± 0.02 eV to fit the spectra

Table 1 The XPS fitting parameters, peak binding energy positions and full width at half maxima (FWHMs) of O_{1s} and $Zn_{2p3/2}$ signals

Core-level electrons	O_{1s}			$Zn_{2p3/2}$	
	LBC, OI	MBC, OII	HBC, OIII	ZnI	ZnII
BE positions (eV)	530.12 ± 0.02	531.47 ± 0.03	532.45 ± 0.02	1021.5	1022.3
FWHMs (eV)	1.61 ± 0.03	1.74 ± 0.02	1.83 ± 0.06	1.89 ± 0.03	2.39 ± 0.08

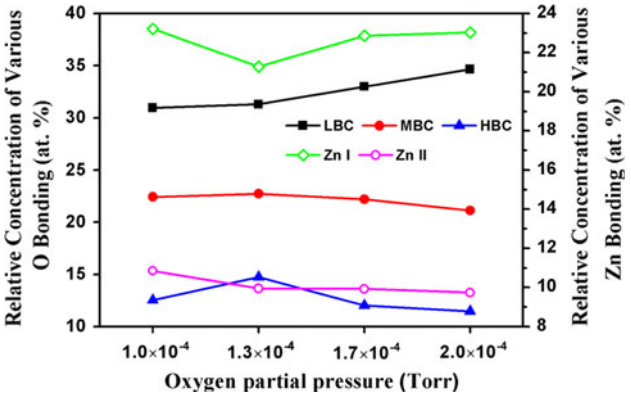

Fig. 8 The relative concentrations of HBC (OIII), MBC (OII), and LBC (OI) components in XPS O_{1s} signal and ZnI and ZnII components in $Zn_{2p3/2}$ signal as functions of oxygen partial pressures were plotted

partial pressure increased. The ZnII decreased as the oxygen partial pressure increased.

The XPS O_{1s} signal can be fitted by three components, located at 530.12 ± 0.02, 531.47 ± 0.03, and 532.45 ± 0.02 eV, respectively as shown in Fig. 7. The high binding energy component (HBC, OIII) located at 532.45 ± 0.02 eV can be attributed to the chemisorbed oxygen, H_2O, or $–CO_3$ on the surface of the film [29–33]. The median binding energy component (MBC, OII) is assigned to the oxygen in the oxygen deficient region [34–36], i.e., oxygen in O-Zn bonds but surrounded by the oxygen vacancies. The MBC was also assigned to OH on the surface in the literature [37, 38]. The dominant low binding energy component (LBC, OI) is originated from the oxygen in the O-Zn bonds [39–42]. The XPS O_{1s} spectra with three components were previously observed in AZO and ZnO films by other researchers [28, 43–45]. The XPS fitting parameters, peak binding energy positions and full width at half maxima (FWHMs) of O_{1s} and $Zn_{2p3/2}$ signals were listed in Table 1. Core-level photoelectrons originated from the bonding elements such as LBC O_{1s} and ZnI have less fluctuation in the position and small FWHMs as shown in Table 1. The relative concentrations of various O_{1s} components and $Zn_{2p3/2}$ components as functions of oxygen partial pressures were plotted in Fig. 8 in which both the OII and ZnII decreased as the oxygen partial pressure increasing. The general trends on the ZnI, OIII, and OI were ZnI and OI increased and OIII decreased as the oxygen partial pressure increasing. Kun Ho Kim et al. pointed out previously that the resistivity of the AZO film was mainly dependent on the carrier concentration [46]. Since the OII is related to the oxygen vacancies and ZnII to Zn interstitials, both decreases indicated the donors were reduced; thus, the low carrier concentration and, therefore, the high resistivity as also detected by Hall measurement shown in Fig. 3.

Conclusion

The AZO films contained 1.5 at.% Al with the low resistivity and high transparency can be obtained by the ion beam co-sputtering deposition without heating substrate during the deposition under 1.3×10^{-4} Torr oxygen partial pressure. The crystallinity is getting worse and the grain sizes become smaller as the various oxygen partial pressures increases. The increase of the resistivity was caused by the decrease of the carrier concentration as oxygen partial pressure increases. Under the optimum oxygen partial pressure of 1.3×10^{-4} Torr the lowest resistivity and the intense (002) peak was observed simultaneously in AZO film. Regardless of the oxygen partial pressure, the average transmittance of AZO films was above 80 % in the visible region; however, the "Red Shift" phenomenon was observed in the UV region as oxygen partial pressure increased due to the Burstein-Moss effect on the optical energy band gap. Finally, the compositions and chemical bonding environment in the films were examined by XPS in which three oxygen components, LBC, MBC, and HBC and two zinc components, ZnI, and ZnII were applied to fit the spectra. Both MBC O_{1s}, related to the oxygen vacancies, and ZnII, related to the Zn interstitials, decreased as the oxygen partial press increased which indicated that the carrier concentration reduced accordingly. Combined to the worse crystallinity, smaller grain size, and lower carrier concentration, as the pressure increasing, it can be concluded that the resistivity of the film enhances as the oxygen partial pressure increases.

Acknowledgements The authors would like to thank Sapintia Culture and Education Foundation, and the National Science Council of Taiwan (grant no. NSC99-2221-E-030-011-MY3) for financially

supporting this study. P. W. Wang appreciates the funding from Bradley University.

References

1. Kim Yumin, Lee Woojin, Jung Dae-Ryong, Kim Jongmin, Nam Seunghoon, Kim Hoechang, Park Byungwoo (2010) Appl Phys Lett 96:171902
2. Ding Jijun, Chen Haixia, Zhao Xinggang, Ma Shuyi (2010) J Phys Chem Solids 71:346
3. Tanusevski Atanas, Georgieva Verka (2010) Appl Surf Sci 256:5056
4. Li C, Furuta M, Matsuda T, Hiramatsu T, Furuta H, Hirao T (2009) Thin Solid Films 517:3265
5. Horwat D, Billard A (2007) Thin Solid Films 515:5444
6. Yang W, Liu Z, Peng DL, Zhang F, Huang H, Xie Y, Wua Z (2009) Appl Surf Sci 255:5669
7. Agura Hideaki, Suzuki Akio, Matsushita Tatsuhiko, Aoki Takanori, Okuda Masahiro (2003) Thin Solid Films 445:263
8. Dong Bin-Zhong, Fang Guo-Jia, Wang Jian-Feng, Guan Wen-Jie, Zhao Xing-Zhong (2007) J Appl Phys 101:033713
9. Sagar Parmod, Kumar Manoj (2005) Thin Solid Films 489:94
10. Studenikin SA (1998) J Appl Phys 84:2287
11. Hsu JC, Lee CC (1998) Appl Opt 37:1171
12. Lee Cheng-Chung, Hsu Jin-Cherng, Wong Daw-Heng (2000) Opt Quant Electron 32:327
13. Chen YY, Hsu JC, Wang PW, Pai YW, Lin YH (2011) Appl Surf Sci 257:3446
14. Chen Y-Y, Hsu J-C, Lee C-Y, Wang PW (2012) Vacuum. http://dx.doi.org/10.1016/j.vacuum.2012.02.054
15. Liquiang J, Yichun Q, Baiqi W, Shudan L, Baojiang J, Libin Y, Wei F, Honggang F, Jiazhong S (2006) Sol Energy Mater Sol Cells 90:1773
16. Vanheusden K, Warren WL, Seager CH, Tallant DR, Voigt JA, Gnade BE (1996) J Appl Phys 79:7983
17. Kang JS, Kang HS, Pang SS, Shim ES, Lee SY (2003) Thin Solid Films 443:5
18. Wang QP, Zhang DH, Xue ZY, Zhang XJ (2004) Opt Mater 26:23
19. Patil AB, Patil KR, Pardeshi SK (2011) J Solid State Chem 184:3273
20. Wei XQ, Man BY, Liu M, Xue CS, Zhuang HZ, Yang C (2007) Physica B388:145
21. Sahdan MZ, Mamat MH, Salina M, Khusaimi Z, Noor UM, Rusop M (2010) Phys Status Solidi C7:2286
22. Kong H, Yang P, Chu J (2011) J Phys, Conference Series 276:012170
23. Huheey JE (1983) Inorganic chemistry, 3rd edn. Harper Collins Publishers, New York, p 73
24. Zeng HB, Duan GT, Li Y, Yang SK, Xu XX, Cai WP (2010) Adv Funct Mater 20:561
25. Xu PS, Sun YM, Shi CS, Xu FQ, Pan HB (2003) Nucl Instrum Meth Phys Res B199:286
26. Look DC, Hemsky JW, Sizelove JR (1999) Phys Rev Lett 82:2552
27. Wagner CD, Riggs WMW, Davis LE, Moulder JF, Mullenberg GE (1979) Handbook of X-ray photoelectron spectroscopy. Perkin-Elmer Corp., Eden Prairie, p 188
28. Lee S, Bang S, Park J, Jeong W, Jeon H (2010) Phys Status Solidi 207:1845
29. Major S (1986) Appl Phys Lett 49:394
30. Nurul Islam Md, Ghosh TB, Chopra KL, Acharya HN (1996) Thin Solid Films 280:20
31. Sanjines R, Coluzza C, Rosenfeld D, Gozzo F, Almeras Ph, Levy F, Margaritondo G (1993) J Appl Phys 73:3997
32. Li LJ, Deng H, Dai LP, Chen JJ, Yuan QL, Li Y (2008) Mat Res Bull 43:1456
33. Kim DK, Kim HB (2011) J Alloy Comp 509:421
34. Wang ZG, Zu XT, Wang LM (2006) Physica E35:199
35. Fan JCC, Goodenough JB (1977) J Appl Phys 48:3524
36. Zhang PF, Liu XL, Wei HY, Fan HB, Liang ZM, Jin P, Yang SY, Jiao CM, Zhu QS, Wang ZG (2007) J Phys D Appl Phys 40:6010
37. Avalle L, Santos E, Leiva E, Macagno VA (1993) Thin Solid Films 219:133
38. Meng LJ, Moreira de Sa CP, dos Santos MP (1994) Appl Surf Sci 78:57
39. Coppa BJ, Davis RF, Nemanish R (2003) Appl Phys Lett 82:400
40. Cebulla R, Werndt R, Ellmer K (1998) J Appl Phys 83:1087
41. Szorenyi T (1995) J Appl Phys 78:6211
42. Rao LK, Vinni V (1993) Appl Phys Lett 63:608
43. Chen M, Wang X, Yu YH, Pei ZL, Bai XD, Sun C, Huang RF, Wen LS (2000) Appl Surf Sci 158:134
44. Chen M, Pei ZL, Sun C, Wen LS, Wang X (2001) Mat Lett 48:194
45. Shi S, Xu J, Zhang X, Li Lan (2011) J Appl Phys 109:103508
46. Kim KH, Park KC, Ma DY (1997) J Appl Phys 81:7764